ISSN 1990-7931, Russian Journal of Physical Chemistry B, 2010, Vol. 4, No. 2, pp. 308–320. © Pleiades Publishing, Ltd., 2010.
Original Russian Text © V.V. Azatyan, S.N. Medvedev, S.M. Frolov, 2010, published in Khimicheskaya Fizika, 2010, Vol. 29, No. 4, pp. 56–69.

COMBUSTION, EXPLOSION, AND SHOCK WAVES

Mathematical Modeling of the Chemical Inhibition of the Detonation of Hydrogen–Air Mixtures

V. V. Azatyan[a], S. N. Medvedev[b], and S. M. Frolov[b]

[a] *Institute of Structural Macrokinetics and Problems of Materials Science, Russian Academy of Sciences, Chernogolovka, Moscow oblast, 142432 Russia*

[b] *Semenov Institute of Chemical Physics, Russian Academy of Sciences, ul. Kosygina 4, Moscow, 119991 Russia*

e-mail: medvedevs@chph.ras.ru

Received July 30, 2009

Abstract—A mathematical modeling of the chemical inhibition of the detonation of hydrogen–air mixtures is performed. It is demonstrated that a one-dimensional model of detonation based on a chain-branching mechanism of hydrogen combustion makes it possible to describe the main regularities of the effect of inhibitors on detonation. The calculation results, which are in good agreement with the available experimental data, show that inhibition causes a narrowing of the concentration limits of detonation and an increase in the critical diameter of detonation.

DOI: 10.1134/S199079311002017X

1. INTRODUCTION

The suppression of explosions of organic compounds with small amounts of additives was observed during tests of internal-combustion piston engines well before the theory of branching-chain reactions appeared [1, 2]. Antiknock additives were methane, hydrogen iodide, organic iodides, and various metalorganic and nitrogen-containing compounds. In [1, 2], the effect of additives was attributed to their ability to prevent the formation and accumulation of organic peroxides and aldehydes, active intermediates of the reaction. The formation of these intermediate products during the oxidation of organic compounds is known to occur by the degenerated chain-branching mechanism at relatively low temperatures (below 800 K), in the region of so-called cool flames (see, e.g., [2]).

In recent times, search for effective anti-detonation additives was resumed in connection with a new stage in the development of hydrogen energetics, largely based on fuel cells. It was demonstrated [3–5] that adding small amounts of inhibitors, including hydrocarbons with unsaturated bonds (olefins), to hydrogen–air mixtures substantially narrows the concentration limits of detonation, increases the predetonation distance, and can even quench a steady detonation wave.

According to these works, the inhibition of the detonation of hydrogen–air mixtures occurs due to an additional chain termination in the chain-branching reaction by the additive. The high efficiency of olefins is associated with a rapid capture of atomic hydrogen by the π bonds of inhibitor molecules.

The authors of [6] systematically examined the predictive possibilities of the one-dimensional theory of detonation limits proposed by Ya.B. Zel'dovich [7–9] by using a detailed kinetic scheme of hydrogen oxidation and refined values of the friction factor and heat transfer coefficient at the tube walls. It was demonstrated that the one-dimensional model satisfactorily predicts the detonation limits as a functions of the composition, initial temperature and pressure, and the type and content of the inert diluent in the hydrogen–air mixture. The aim of the present work was to apply the model developed in [6–9] to the problem of detonation inhibition in hydrogen–air mixtures with small amounts of effective anti-detonation additives.

2. FORMULATION OF THE PROBLEM

2.1. Physical Formulation of the Problem

Let a steady planar detonation wave propagate in a straight channel of diameter d filled with a mixture of reactive gases. As in [6–9], the following simplifying assumptions were made:

(1) the flow behind the detonation wave is one-dimensional;

(2) the structure of the detonation wave is the same as in the Zel'dovich–von Neumann–Doering model;

(3) the reaction mixture obeys the equations of state of an ideal gas;

(4) isothermal conditions are specified at the tube wall;

(5) the parameters of the flow change in the transversal direction only due to friction and heat transfer at the tube wall;

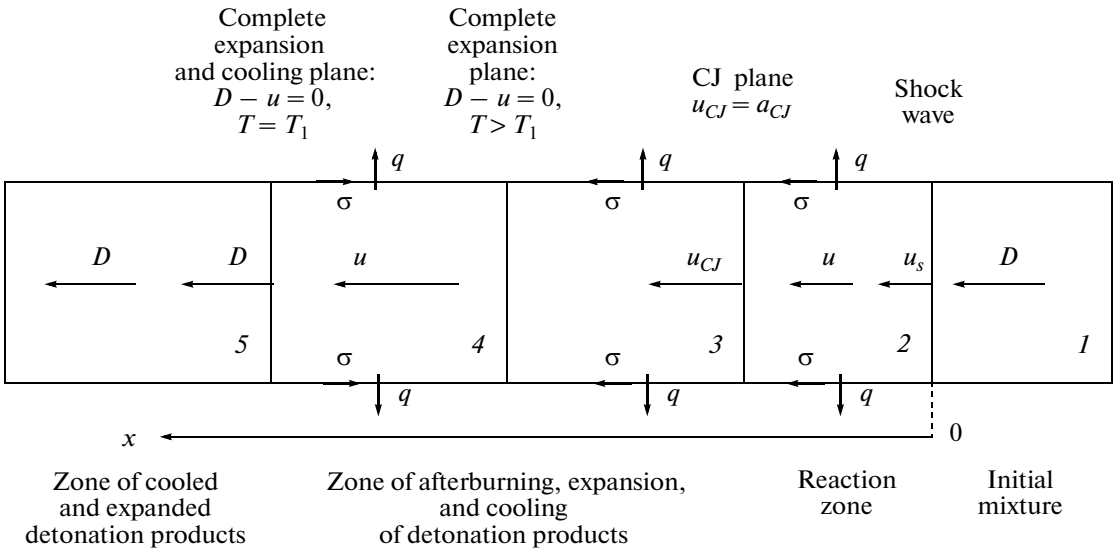

Fig. 1. Structure of a steady detonation wave.

(6) the friction factor and heat transfer coefficient are related by the Reynolds analogy;

(7) the contribution from light emission is negligibly small;

(8) the chemical reaction rate is constant across the channel.

A scheme of the flow in the system of coordinates attached to the front of the leading shock wave ($x = 0$) is displayed in Fig. 1. The x axis is directed downstream of the flow. According to the theory developed in [7–9], the entire flow region was divided into five zones (*1*)–(*5*). In this system of coordinates, the tube wall moves at a velocity D and has a temperature T_1.

Zone *1* is occupied by a uniform initial mixture with density ρ_1, pressure p_1, and temperature T_1, which flows onto the shock wave front at the detonation velocity D.

Zone *2* is the reaction zone, in which the initial mixture is first instantaneously adiabatically compressed in the shock wave (the density, pressure, and temperature increases from ρ_1, p_1, and T_1 to ρ_s, p_s, and T_s (the subscript s denotes the parameters of the gas immediately behind the shock wave front), whereas the flow velocity decreases from D to u_s, which is always smaller than the local speed of sound, $u_s < a_s$). Then, after a certain induction period, the mixture self-ignites and gradually burns out. It is known that the heat input from the reaction into a subsonic flow accelerates it to a velocity of $u_2 = u_{CJ}$ (the subscript CJ denotes the parameters of the gas at the Chapman–Jouguet point). At the CJ point, an important condition is fulfilled: the gas flow velocity is identical to the local speed of sound $u_{CJ} = a_{CJ}$. This condition (CJ condition) ensures the stability of the detonation wave, since small perturbations arising downstream from the front does not reach the reaction zone. The temperature in the reaction zone increases from T_2 to T_{CJ}, whereas the density and pressure decrease to $\rho_2 = \rho_{CJ}$ and $p_2 = p_{CJ}$. Since the temperature T_2 is higher than the temperature of the tube wall T_1, a heat flux q from the reaction zone to the wall arises; i.e., the flow in zone *2* is essentially nonadiabatic. In addition, since $u_2 < D$, the tube wall does external work on the gas because of a nonzero viscous friction stress σ, which is directed downstream of the flow (Fig. 1). In contrast to the heat released by the reaction, the heat transfer to the wall and the external work done on the gas cause a deceleration of the subsonic flow, i.e., impede the gas from achieving the Chapman–Jouguet condition and thereby predetermine the existence of the detonation limits. The factors that prevent the gas from achieving the CJ point in the reaction zone of the detonation wave are normally termed "losses", more specifically, heat and momentum losses. Note that, because of the competitive action of the above-mentioned physicochemical processes on the flow in the reaction zone of the detonation wave, the chemical transformations at the CJ point remain uncompleted.

In zones *3* and *4*, the afterburning of the mixture and the expansion and cooling of the detonation products occur. In zone *3*, under the action of the external work done on the gas and of the heat transfer to the tube wall, the supersonic flow accelerates from $u_3 = u_{CJ}$ to $u_3 = D$; i.e., a complete expansion of the gas from the density of $\rho_3 = \rho_{CJ}$ to the density of the initial mixture, $\rho_3 = \rho_1$, occurs. Clearly, the afterburning of the mixture in zone *3* to some extent impedes the acceleration of the supersonic flow. Since the gas

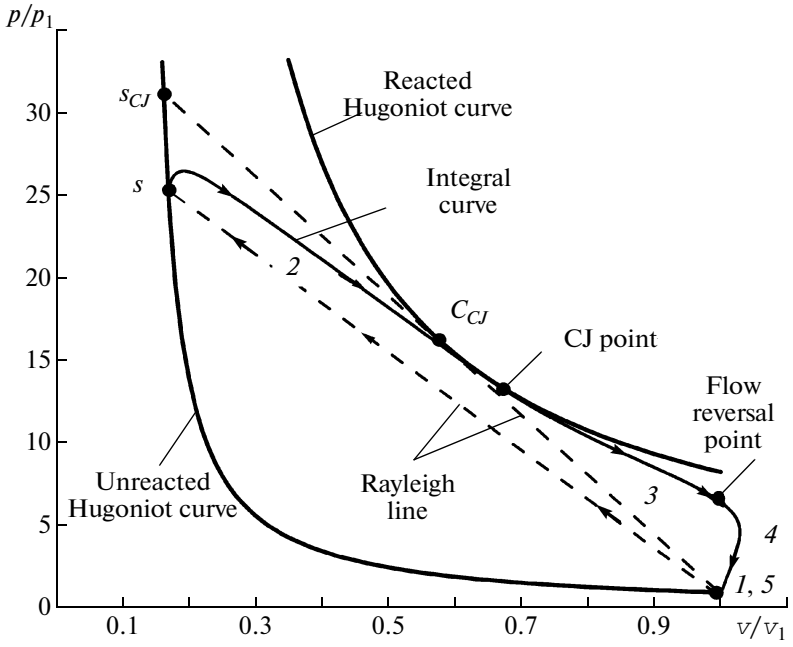

Fig. 2. Changes in the state of the gas in the detonation wave illustrated in the pressure–specific volume plane.

temperature at the end of zone *3* still differs from the temperature of the wall ($T_3 > T_1$), the cooling of the gas continues. In zone *4*, the supersonic gas flow first continues to accelerate to a velocity of $u_4 > D$ due to the predominant influence of cooling and then decelerates to a velocity of $u_4 = D$ due to the predominant influence of viscous stress at the wall, which reverses its direction in zone *4* if $u_4 > D$ (Fig. 1).

In zone *5*, the detonation products have the density and temperature identical to those of the initial mixture and flow at a velocity D. The pressure in zone *5* may somewhat differ from the pressure p_1 if the number of moles of gas changes after the chemical reaction.

Based on the results from [9], we plotted Fig. 2, where the arrows show the changes in the state of the gas in the detonation wave in the pressure–specific volume plane. As can be seen, in the presence of losses, the state of the gas changes along curve *1–s–2–3–4–5*, with the transition from state *1* to state *s* occurring stepwise. Recall that, in the ZND theory of ideal detonation, the state of the gas changes along the Rayleigh line, line $1–s_{CJ}–C_{CJ}$, where C_{CJ} is the classical CJ point, the point of tangency of the Rayleigh line and the Hugoniot curve. In the presence of momentum and energy losses, the CJ point is positioned below and to the right of the classical CJ point for ideal detonation, generally outside the Hugoniot curve corresponding to the thermodynamically equilibrium detonation products at the given initial conditions.

Thus, the detonation wave region encompasses zones *2*, *3*, and *4*. To solve the problem of inhibition of the detonation of hydrogen–air mixtures with small amount of effective anti-detonation additives, it is necessary to consider the flow in all these zones.

2.2. Mathematical Formulation of the Problem

The governing equations of the model include [6–9]:
The mass conservation equation

$$\frac{d\rho u}{dx} = 0. \tag{1}$$

The species conservation equation

$$\frac{d\rho_i u}{dt} = \chi_i \mu_i, \quad \rho_i = c_i \mu_i$$

$$\chi_i = \sum_{j=1}^{L} \beta_{ij} r_j, \tag{2}$$

$$r_j = k_f \prod_{l=1}^{n} c_l - k_r \prod_{l=1}^{m} c_l.$$

The momentum conservation equation

$$\frac{d}{dx}\left(p + \rho u^2\right) = \frac{\Pi}{\Phi}\sigma. \tag{3}$$

The energy conservation equation

$$\rho u \frac{d}{dx}\left[\frac{u^2}{2} + \frac{1}{\rho}\left(\sum_{i=1}^{N} H_i c_i\right)\right] = \frac{\Pi}{\Phi}(\sigma D - q). \tag{4}$$

In Eqs. (1)–(4), c_i, μ_i, and H_i are the molar concentration, molecular mass, and enthalpy of the ith chemical species of the mixture, L is the total number of

chemical reactions occurring in the mixture, β_{ij} is the stoichiometric coefficient of the ith component in the jth reaction, N is the total number of species in the mixture, k_f and k_r are the rate constants for the forward and reverse reactions, and Π and Φ are the perimeter and cross sectional area of the tube.

The reaction rate constants k_f and k_r were calculated by the formula

$$k = AT^n \exp(-E/RT), \tag{5}$$

where E is the activation energy, A is the preexponential factor, and n is the temperature exponent.

The system of equations (1)–(4) was supplemented with the equation of state for a mixture of ideal gases:

$$p = \sum_{i=1}^{N} \rho_i RT, \tag{6}$$

where R is the universal gas constant. The expressions for the viscous stress σ and heat flux q read as

$$\sigma = \frac{1}{2} C_f \rho (D-u)|D-u|, \quad C_f = \frac{0.3164}{\mathrm{Re}^{0.25}}, \tag{7}$$

$$q = C_h \rho (D-u)\left[C_p(T-T_1) + \frac{1}{2}(D-u)^2\right], \quad C_h = \frac{1}{2}C_f. \tag{8}$$

In Eqs. (6)–(8), C_f is the friction factor given by the Blasius formula, C_h is the dimensionless heat transfer coefficient determined from the Reynolds analogy, C_p is the heat capacity of the mixture at constant pressure, and Re is the Reynolds number calculated by the formula

$$\mathrm{Re} = \frac{\rho_1 (D-u) d}{\eta_1}, \tag{9}$$

where d is the tube diameter and η_1 is the dynamic viscosity of the mixture [10]:

$$\eta_1 = 26.7 \times 10^{-7} \frac{(\mu_1 T_1)^{0.5}}{\sigma_m^2}. \tag{10}$$

Here, σ_m is the hard-sphere radius of the mixture species, and μ_1 is the molecular mass.

To solve the system of differential equations (1)–(4), it is necessary to formulate the boundary conditions at the shock wave front (at $x = 0$) and at a large distance from the wave ($x \to \infty$). The boundary conditions at the shock wave front correspond to the Rankine–Hugoniot conditions:

$$\begin{gathered} \rho_s u_s = \rho_1 D, \\ p_s + \rho_s u_s^2 = p_1 + \rho_1 D^2, \\ \frac{1}{\rho_s}\left(\sum_{i=1}^{N} H_i c_i\right)_s + \frac{u_s^2}{2} = \frac{1}{\rho_1}\left(\sum_{i=1}^{N} H_i c_i\right)_1 + \frac{D^2}{2}, \\ (c_i)_s = (c_i)_1. \end{gathered} \tag{11}$$

At a large distance from the wave, the following conditions should be satisfied:

$$x \to \infty: \quad \rho \to \rho_1; \quad T \to T_1. \tag{12}$$

In this formulation, the detonation velocity D is the eigenvalue of the problem, which is determined by using the shooting method [6].

2.3. Kinetic Mechanism

To describe the effect of inhibitors on the detonation of hydrogen–air mixtures, it is necessary to use kinetic mechanisms including the main steps of the branching-chain oxidation of hydrogen with the known rate constants and thermodynamic data. The kinetic mechanism of hydrogen oxidation used in the present work is presented in the table. The mechanism consists of 21 reactions (I–XXI) involving 8 species (H_2, O_2, OH, H_2O, H, O, HO_2, H_2O_2); M denotes any species. The relevant thermodynamic data were borrowed from [11].

The inhibitor of the detonation of hydrogen–air mixtures was propene (C_3H_6). The effect of propene was modeled by the following two reactions added to the kinetic mechanism given in the table:

$$C_3H_6 + H(+M) \to C_3H_7(+M) \qquad \text{(XXII)}$$

and

$$C_3H_7 + O_2 \to C_3H_6 + HO_2. \qquad \text{(XXIII)}$$

Reaction (XXII) is chain termination via the addition of a hydrogen atom to a C_3H_6 molecule with the formation of the less active propyl radical (C_3H_7). Due to the high frequency of triple collisions at atmospheric and higher pressures, reaction (XXII) obeys the second-order kinetic law, with the rate constant given by l/(mol s)

$$k = 1.3 \times 10^{10} \exp\left(-\frac{787.87}{T}\right) \text{l/(mol s)}. \tag{13}$$

A comparison of the rate constants for reactions (XXII) and (III) shows that, if only several tenths of a percent of propene are present in a hydrogen–air mixture, chain-termination reaction (XXII) effectively competes with chain-branching reaction (III). Note that propene reacts not only with hydrogen atoms but also with oxygen atoms and hydroxyl radicals; therefore, the use of only reaction (XXII) underestimates the chain termination rate, since the reac-

Kinetic mechanism of hydrogen oxidation

Reaction no.	Reaction	Forward			Reverse		
		log*A* [cm mol s]	*n*	*E*, kcal/mol	log*A* [cm mol s]	*n*	*E*, kcal/mol
I	$H_2 + O_2 = OH + OH$	13.24	0	48.1	10.82	0.3	29.2
II	$OH + H_2 = H_2O + H$	8.00	1.6	3.30	8.66	1.6	18.57
III	$H + O_2 = OH + O$	17.08	−0.9	16.52	13.25	0	0
IV	$O + H_2 = OH + H$	7.18	2.0	7.55	3.69	2.8	3.88
V	$O + H_2O = OH + OH$	10.18	1.1	17.26	9.18	1.1	0
VI	$H+H + M = H_2 + M$	17.81	−1.0	0	18.77	−1.1	104.4
VII	$H + O_2 + M = HO_2 + M$	17.85	−0.8	0	19.06	−1.2	48.41
VIII	$OH + H + M = H_2O + M$	21.92	−2.0	0	15.11	0	105.1
IX	$HO_2 + H_2 = H_2O_2 + H$	13.48	0	26.03	13.68	0	7.95
X	$HO_2 + HO_2 = H_2O_2 + O_2$	12.26	0	0	13.73	0	39.74
XI	$H + HO_2 = OH + OH$	14.40	0	1.9	13.08	0	40.1
XII	$H + HO_2 = H_2O + O$	13.15	0	2.08	12.74	0	57.53
XIII	$H + HO_2 = H_2 + O_2$	13.82	0	2.13	14.16	0	56.64
XIV	$O + HO_2 = OH + O_2$	13.24	0	−0.4	13.35	0	52.66
XV	$OH + HO_2 = H_2O + O_2$	13.48	0	0	14.60	0	73.0
XVI	$OH + OH + M = H_2O_2 + M$	24.76	−3.0	0	33.11	−4.9	53.25
XVII	$HO_2 + H_2 = H_2O + OH$	11.78	0	18.68	11.44	0	73.74
XVIII	$HO_2 + H_2O = H_2O_2 + OH$	13.40	0	32.29	13.06	0	1.76
XIX	$H + H_2O_2 = H_2O + OH$	13.38	0	3.97	14.06	0	79.19
XX	$OH + M = O + H + M$	15.38	0	99.36	18.67	−1.0	0
XXI	$O + O + M = O_2 + M$	13.28	0	−1.79	18.26	−1.0	118.1

tions of C_3H_6 with O and OH also result in the substitution of low-active radicals for active species.

Reaction (XXIII) is the regeneration of propene through the interaction of propyl radicals with molecular oxygen. This reaction proceeds in two steps [12–15]:

$$C_3H_7 + O_2 = C_3H_7O_2,$$

followed by the isomerization of the $C_3H_7O_2$ molecule and the subsequent abstraction of HO_2,

$$C_3H_7O_2 = C_3H_6 + HO_2.$$

Note that the formation of HO_2 radicals by the reaction of propyl radicals with O_2 was observed during the inhibition of hydrogen combustion by this hydrocarbon [14, 15]. In this experiment, the introduction of a small amount of inhibitor caused a reduction in the intensity of combustion, decreases in the concentrations of H, O, and OH, and, an increase in the HO_2 concentration. The spectra of atoms and radicals in the flame were recorded with LMR and EPR spectrometers.

The rate constant of reaction (XXIII) was set equal to

$$k = 1.26 \times 10^8 \text{ l/(mol s)}. \quad (14)$$

3. SOLUTION OF THE PROBLEM

3.1. Numerical Method

The system of nonlinear differential equations (1)–(4) together with relationships (5)–(14) was reduced to a dimensionless form using the notations:

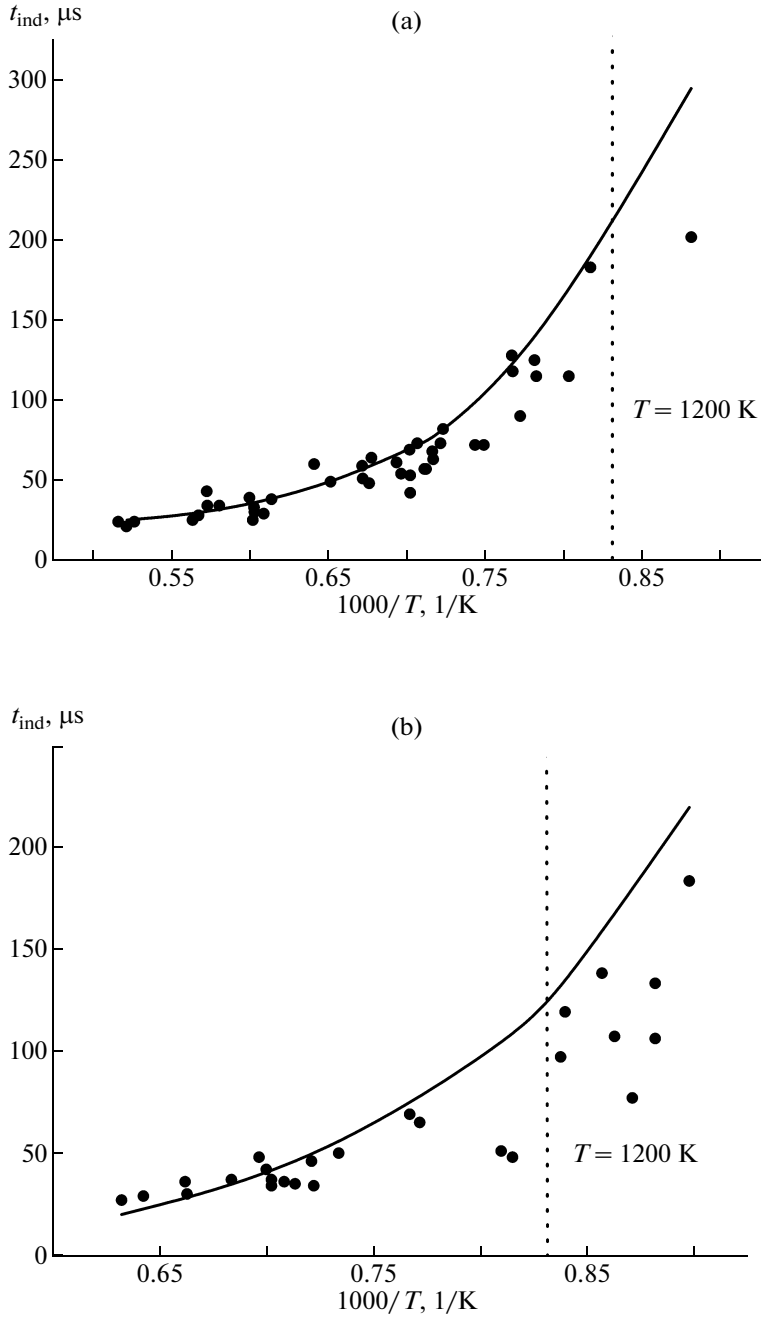

Fig. 3. Calculated (curves) and measured (symbols) dependences of the ignition delay time on the temperature for hydrogen–air mixtures at (a) $[H_2] = 5$ vol % and $p_1 = 0.0211–0.0436$ MPa and (b) $[H_2] = 20$ vol % and $p_1 = 0.0215–0.0346$ MPa.

$$S = \frac{v_1 d\Pi}{C_1^2 \Phi}\sigma;\ W = \frac{v_1 d\Pi}{C_1^2 \Phi D} q;\ \mathrm{Ma} = \frac{D}{C_1};\ P = \frac{p}{p_1};\ V = \frac{v}{v_1};$$
$$\tau = \frac{C_1}{d} t;\quad \xi = \frac{x}{d};\quad \dot{Q} = \frac{dQ}{dt}\frac{d}{C_1^3}, \tag{15}$$

where v_1 is the specific volume, C_1 is the speed of sound in the gas in zone *1* (Fig. 1), and $\dot{Q}$ is the rate of heat release by the chemical reactions.

In the dimensionless form, the system of governing equations reads as

$$\frac{dV}{d\xi} = \frac{1}{\mathrm{Ma}^2}\frac{f' - f''}{\psi},$$
$$\frac{dP}{d\xi} = \gamma_1 \frac{f' - f''(1-\psi)}{\psi}, \tag{16}$$

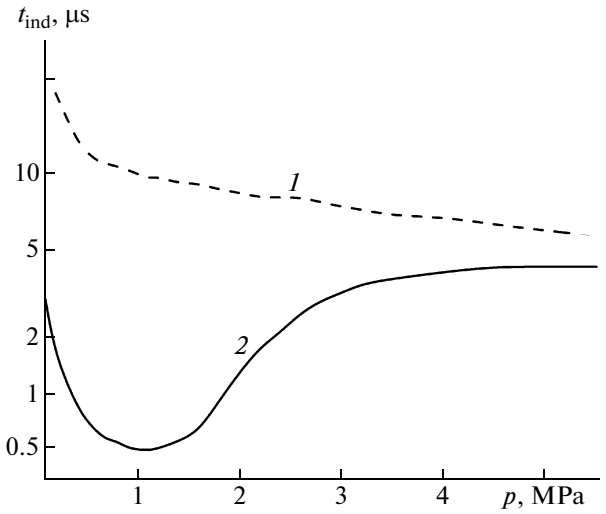

Fig. 4. Calculated dependences of the ignition delay time on the initial pressure p_1 for a stoichiometric hydrogen–air mixture with (1.0 vol %, curve *1*) and without (curve *2*) inhibitor. The initial temperature, $T_1 = 1200$ K.

where

$$\psi = 1 - \frac{\gamma P}{\gamma_1 \mathrm{Ma}^2 V},$$

$$f' = S,$$

$$f'' = (\gamma - 1)\left(S\frac{1-V}{V} - \frac{W}{V}\right) - (\gamma - 1)\frac{\sum \dot{Q}_i}{\mathrm{Ma}V^2}.$$

Here, the parameters S and W describe, respectively, the rates of momentum and heat losses.

The variable $\varphi = f' - f''$ is proportional to the difference between the rates of heat release and heat losses, whereas ψ is the difference between the local flow velocity and sound speed. The conditions at which the variables φ and ψ simultaneously become equal to zero,

$$\frac{dV}{d\xi} = \frac{0}{0}, \quad \frac{dP}{d\xi} = \frac{0}{0}, \tag{17}$$

correspond to the generalized Chapman–Jouguet condition, which was first suggested by Ya.B. Zel'dovich [7, 8]. The singular point in Eqs. (16) is of saddle type, and, therefore, to solve the problem with boundary conditions (12), it is necessary to ensure a continuous transition through the singular point into the region of supersonic flow. This transition is possible only at a certain value of the detonation velocity D. Therefore, instead of boundary conditions (12), we used the condition of continuous transition through this singular point.

In the course of numerical solution of the problem, the value of D was determined by the shooting method, as in [6], i.e., by integrating system (16) together with the kinetic equations and the additional relationships at various D until both conditions (17) were met. The problem was solved by the fourth-order Runge–Kutta method. The system of kinetic equations was solved by the matrix-exponential method [16] with internal integration step. The relative accuracy of calculating the detonation velocity was within 0.05%.

The effect of an inhibitor on the structure of the detonation wave and on the detonation limits was examined for small additives (1 and 2 vol %) of propene C_3H_6, as an example. Such concentrations of propene are smaller than the lower concentration limit of flame propagation in the absence of hydrogen at an initial temperature of 293 K. In the presence of H_2, the hydrocarbon reacts with the atoms and radicals formed in the flame; therefore, part of the oxygen is spent on reactions involving the radicals formed from the C_3H_6 molecule.

3.2. Tests of the Kinetic Mechanism

To test the selected mechanism, we calculated the ignition delay times for hydrogen–air mixtures of various compositions at different initial conditions. The calculation results were compared to the available experimental data. In Figs. 3a and 3b, the symbols represent the experimental data from [17] for hydrogen–air mixtures containing 5 and 20 vol % hydrogen, respectively, whereas the curves show the corresponding calculation results. The vertical dashed line indicates the temperature 1200 K. All the points to the left of this line correspond to temperatures realized in detonation waves in hydrogen–air mixtures. As can be seen, the calculation results are in close agreement with the experimental data.

3.3. Detonation Limits

The main effect of a detonation inhibitor is to increase the autoignition delay time. Figure 4 shows calculated dependences of t_{ind} for a stoichiometric hydrogen–air mixture with (curve *1*) and without (curve *2*) propene additive on the initial pressure at 1200 K. As can be seen, the behavior of the upper curve qualitatively differs from that behavior of the lower curve. For the mixture containing the inhibitor, the ignition delay time decreases monotonically with increasing initial pressure, at least within $p_1 = 0.1$–

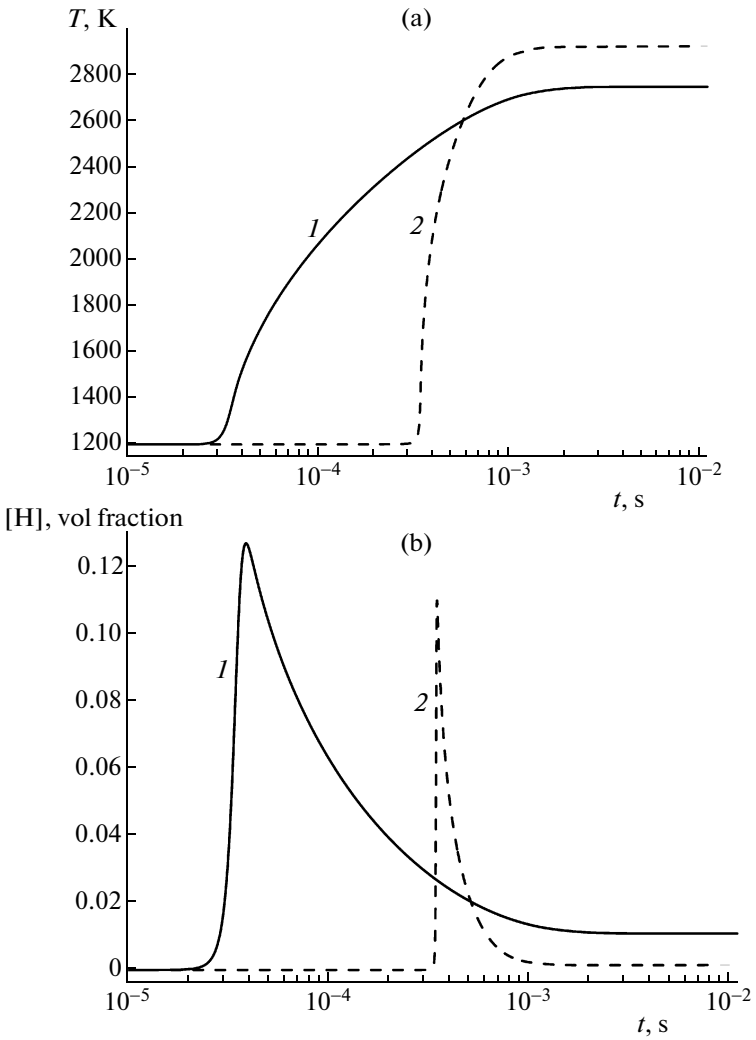

Fig. 5. Calculated time profiles of (a) temperature and (b) [H] concentration for the autoignition of (*1*) 29.6% H_2– 70.4% air and (*2*) 29.6 H_2–1.0% C_3H_6 + 69.4% air mixtures at initial conditions of $T_1 = 1200$ K and $p_1 = 0.1$ MPa.

5.0 MPa. At pressures above 5.0 MPa, the curves converge; i.e., the efficiency of the inhibitor decreases.

Figure 5 shows the calculated time profiles of the temperature and atomic hydrogen concentration at an initial pressure of 0.1 MPa, with the rest of the conditions being specified in the caption of Fig. 4. As can be seen, the ignition delay times differ by an order of magnitude. The final temperature of the mixture with the inhibitor is nearly 200 K higher than that of the mixture without the inhibitor, which can be explained by the occurrence of the exothermic process of formation of HO_2 radicals through reactions (XXII) and (XXIII).

Curve *2* in Fig. 5b shows that the maximum concentration of atomic hydrogen is by ~20% lower than that observed for the autoignition of the inhibitor-free mixture. Moreover, in the inhibitor-containing mixture, atomic hydrogen exists for a substantially shorter time as compared to the inhibitor-free mixture. These observations are manifestations of the inhibition of the process.

Figure 6 shows the time histories of the $[C_3H_6]$ concentration and the concentrations of a number of radicals. Within the initial portion of the time history, $[C_3H_6]$ concentration remains nearly constant, but propyl radicals C_3H_7 appear and accumulate starting from the very beginning of the process, an observation indicative of the reaction of C_3H_6 with atomic hydrogen (one of the main chain carriers of the chain-branching process). The inhibitor is regenerated with the formation of HO_2 radicals. For comparison, Fig. 6 displays the kinetic curves for $[HO_2]$ in the presence and absence of the inhibitor. Note that the inhibitor is regenerated only partially, since it participates in other reactions [13]. However, this circumstance does not affect the main conclusions of the present work.

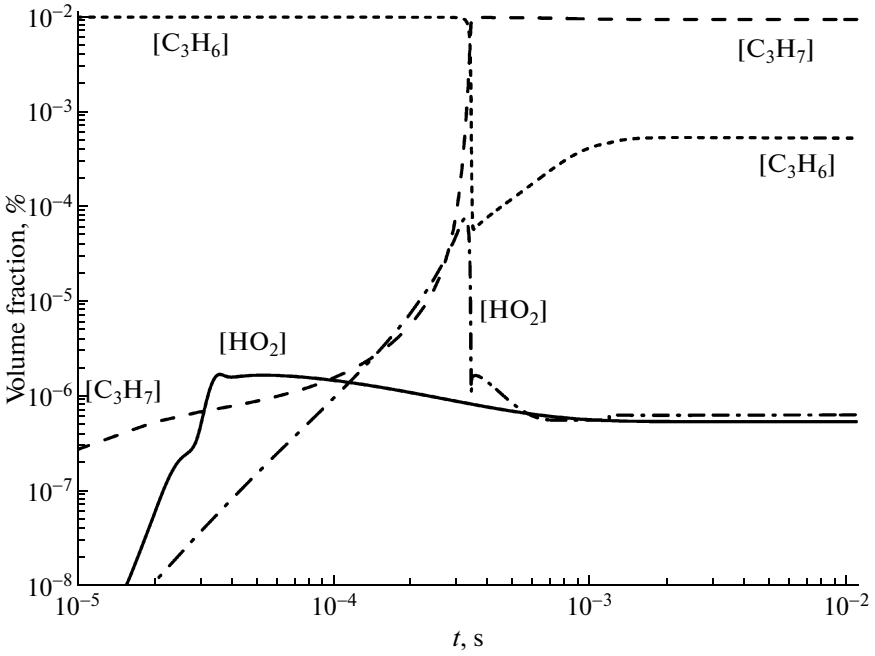

Fig. 6. Calculated time histories of the $[C_3H_6]$, $[C_3H_7]$, and $[HO_2]$ concentrations for the autoignition of a stoichiometric hydrogen–air mixture without (solid line) and with (1 vol % C_3H_6) inhibitor (dashed lines) at initial conditions of $T_1 = 1200$ K and $p_1 = 0.1$ MPa.

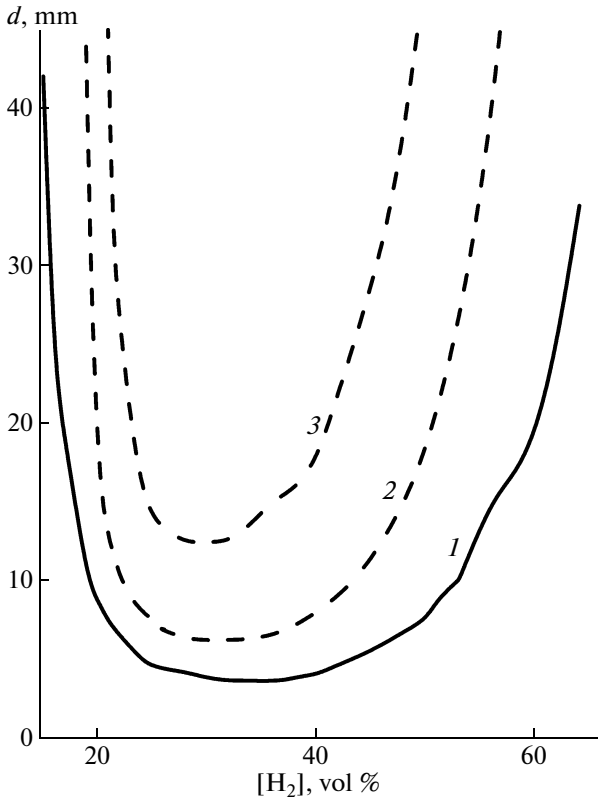

Fig. 7. Calculated dependences of the limiting diameter of detonation on the hydrogen concentration. The curves correspond to different amounts of inhibitor added: (*1*) 0, (*2*) 1.0, and (*3*) 2.0 vol % at initial parameters of the system of $T_1 = 298$ K and $p_1 = 0.1$ MPa.

Addition of an inhibitor results in a narrowing of the concentration limits and in an increase of the minimum channel diameter in which the detonation wave still propagates. The calculated dependences of the limiting diameter of the tube on the hydrogen content in the hydrogen–air mixture without and with the inhibitor (in concentrations of 1 and 2% propene) are displayed in Fig. 7. All the curves have a U-shaped form and make it possible to determine the detonation concentration limits at a given diameter of the channel. Curve *1* closely reproduces the calculation results reported in [6]. Note that the authors of [6] compared their calculation results with the experimental data from [18, 19] and revealed a satisfactory qualitative and quantitative agreement. The theory predicts that the minimum (limiting) channel diameter at which steady detonation can still propagate in a hydrogen–air mixture is 3.7 mm. Figure 7 shows that, upon addition of 1% propene to a hydrogen–air mixture in a 20-mm-diameter tube, the lean detonation limit shifts from 16.9 to 19.76 vol % whereas the rich limit shifts from 60.05 to 50.63 vol %. Upon addition propene, the limiting diameter of the tube increases from 3.7 mm (without inhibitor) to 6.3 mm and 12.5 mm at 1 and 2 vol % propene, respectively. In addition, upon introduction of the inhibitor, the minimum of the U-shaped curves shifts to lower hydrogen concentrations.

An analysis of the data presented in Fig. 7 led us to another important conclusion: even in large-diameter tubes, in which momentum and energy losses can be

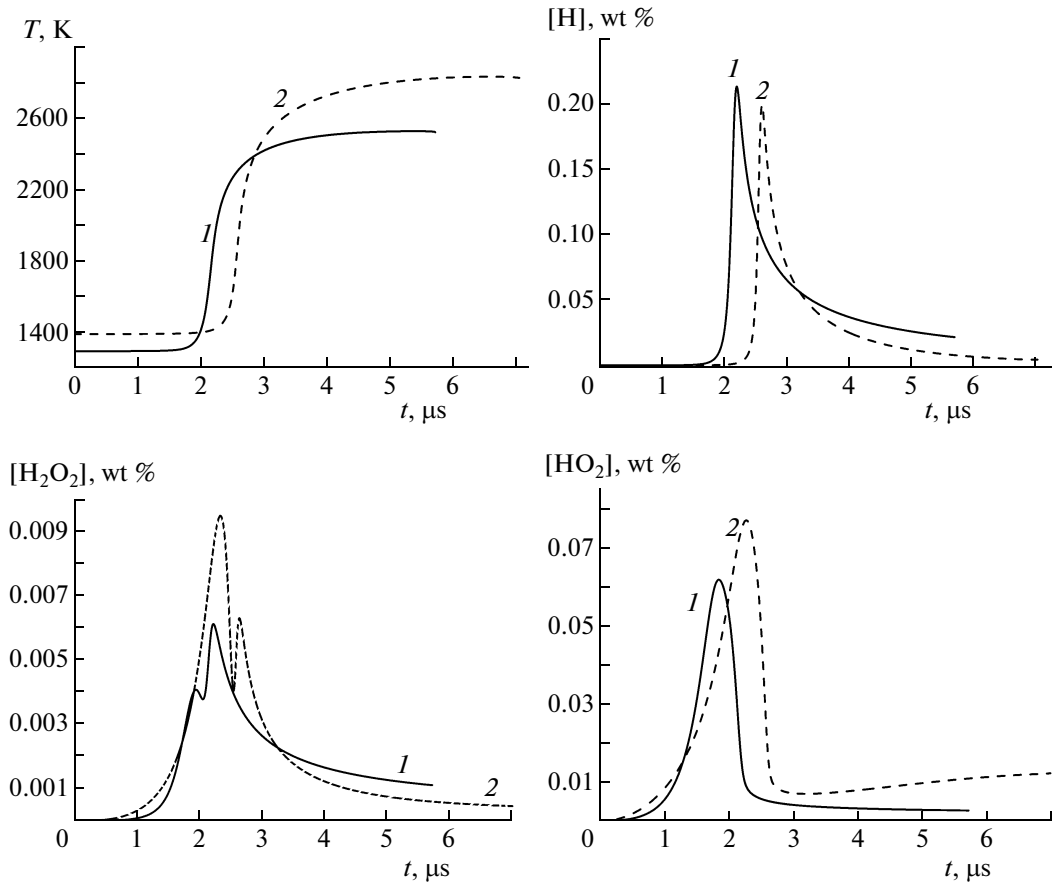

Fig. 8. Calculated time profiles of the temperature and mass fractions of [H], [HO_2], and [H_2O_2] for (*1*) 22 vol % H_2–78 vol % air and (*2*) 22 vol % H_2–1.0 vol % C_3H_6–77 vol % air mixtures at initial parameters of the system of $T_1 = 298$ K and $p_1 = 0.1$ MPa.

disregarded, propene additives influence the concentration limits of detonation. Indeed, addition of 1% inhibitor results in a narrowing of the lean and rich detonation limits, by 3 and 8% in H_2, respectively; at 2% inhibitor, the corresponding values are 6.0 and 16%.

3.4. Detonation Structure

Let us consider how inhibitor additives influence the structure of the reaction zone of the detonation wave. Figure 8 shows the calculated time profiles of the temperature, specific volume, and concentrations of H, HO_2, and H_2O_2 in detonation waves propagating in near-critical mixtures without and with (1%) inhibitor. Calculations were performed for tubes 6 and 9 mm in diameter. Note that the calculated time profiles of the pressure and density feature no irregularities, and therefore, they are not shown. The calculation results displayed in Fig. 8 refer to a 22 vol % hydrogen–air mixture at an initial temperature of $T_1 = 298$ K and an initial pressure of $p_1 = 0.1$ MPa. The temperatures at the front of the leading shock wave in the two mixtures differ because of the difference in the detonation velocity: $D = 1681.5$ m/s (curve *1*) and 1748.4 m/s (curve *2*), which can be explained by a higher enthalpy of formation of the inhibitor. Generally, in both cases, the temperature profiles are qualitatively similar. Note, however, that, in the mixture with inhibitor, the atomic hydrogen concentration is substantially lower whereas the concentrations of less active species, HO_2 and H_2O_2 are markedly higher.

The calculated dependences of the detonation velocity on the hydrogen concentration in the mixture with and without inhibitor are shown in Fig. 9. As is seen, near the concentration limits, the limiting detonation velocity only slightly differs from D_{CJ}: $\Delta D/D_{CJ} = 4$–5% at the lean limit and $\Delta D/D_{CJ} = 8$–10% at the rich limit. The maximum decrease in the detonation velocity, $\Delta D/D_{CJ} = 15\%$, was observed for mixtures containing 35–45 vol % hydrogen. Upon addition of the inhibitor the concentration limits narrow and the velocity decrease also diminishes (Fig. 9, curve *2*). For example, upon addition of 1 vol % C_3H_6, the admissible change in the detonation velocity at the lean and rich limits turned out to be close to $\Delta D/D_{CJ} = 2$–3 and 3–4%, respectively, whereas the

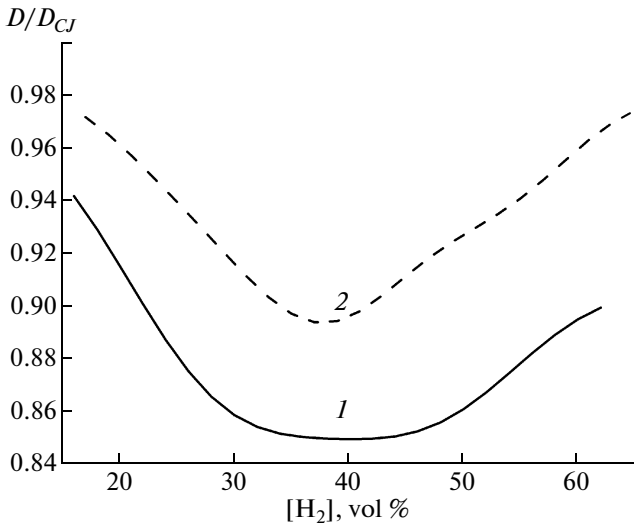

Fig. 9. Calculated dependences of the detonation velocity on the $[H_2]$ concentration for (*1*) H_2–air and (*2*) H_2–air–1% C_3H_6 mixtures at initial parameters of the system of $T_1 = 298$ K and $p_1 = 0.1$ MPa.

maximum decrease in the detonation velocity was $\Delta D/D_{CJ} < 11\%$.

4. EXPERIMENTAL STUDIES

The results of experimental studies of the inhibition of the detonation of hydrogen–air mixtures by small amounts of hydrocarbons are presented in [5]. Figure 10 shows a schematic of the experimental setup used in [5]: a straight detonation tube, 101 mm in diameter and 15 m in length, equipped with detonation initiation, gas handling, and measuring units. At a number of positions along the tube, a pressure transducer and a photodiode opposite it were installed.

The initiation section was a variable-cross-section narrow tube attached to the detonation section. The experimental procedure was as follows. First, the initiation and detonation sections were evacuated and then filled with the working hydrogen–air mixture. The working mixture was introduced through an inlet located at the middle of the tube to a pressure 0.8–0.95 atm, after which the initiation section was filled through the inlet at its end face with a stoichiometric hydrogen–oxygen mixture to a total pressure of 1 atm. During such introduction, the hydrogen–oxygen mixture displaced the working hydrogen–air mixture from the initiation section and from a lead-in part of the detonation section, by 0.9–1.0 m from the junction between the sections. Detonation was initiated near the end face of the initiation section with a 3-J electric discharge. The detonation wave passed from the initiation section into the detonation section propagated there. The detonation velocity was calculated from the recordings of the signals from the pressure transducers and photodiodes.

The working mixture was composed of 33.8% H_2 and air. In mixtures containing no inhibitor, detonation propagated at a velocity of 1980 m/s, very close to the CJ detonation velocity for this mixture. This detonation velocity settled at a distance of 2.0–2.5 m from the detonation section entrance. Figure 11 shows the distance–time diagrams for four experiments with the same initial condition; as can be seen, the results are well reproducible. The pressure and light emission signals at each cross section deviated from the base line simultaneously, an observation that, together with the measured wave velocity, is indicative of the detonation mode of wave propagation.

The detonation inhibitors in [5] were isobutene and propene. At an inhibitor content of 3 vol % and higher, no detonation in a 33.8% hydrogen–air mixture was observed, all other things being equal: the reaction

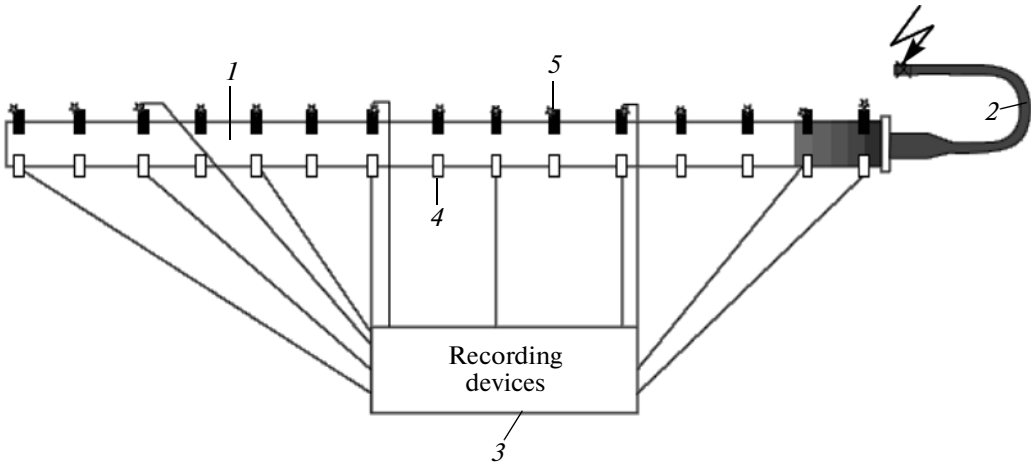

Fig. 10. Schematic of the experimental setup used in [5]: (*1*) detonation tube, (*2*) detonation initiation section, (*3*) recording devices, (*4*) pressure transducers, and (*5*) photodiodes.

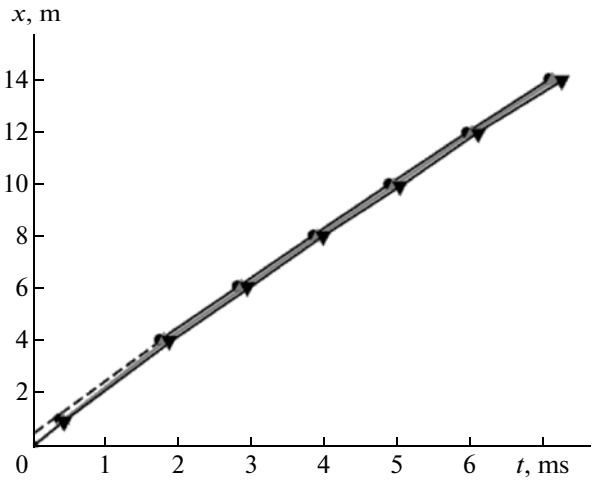

Fig. 11. Distance–time diagram for detonation propagation in a 33.8% H_2–air mixture as measured in four experiments at the same initial conditions [5].

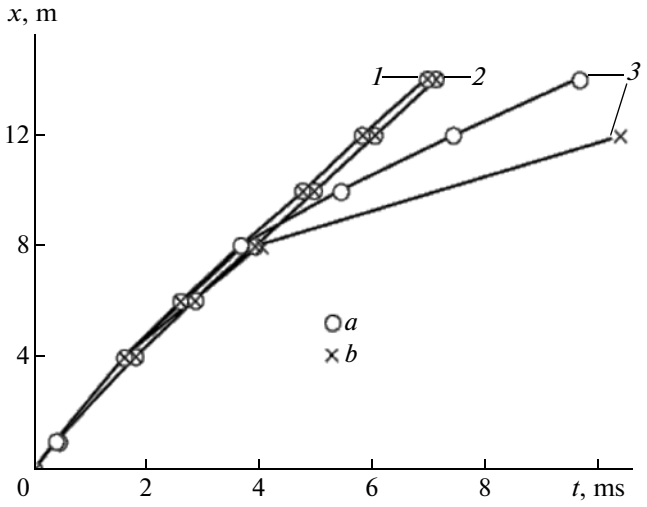

Fig. 12. Distance–time diagram for (*a*) shock wave and (*b*) reaction front propagation in 33.8% H_2–air mixtures (*1*) without and (*2, 3*) with inhibitor in concentrations of (*2*) 2.0 and (*3*) 2.2 vol % [5].

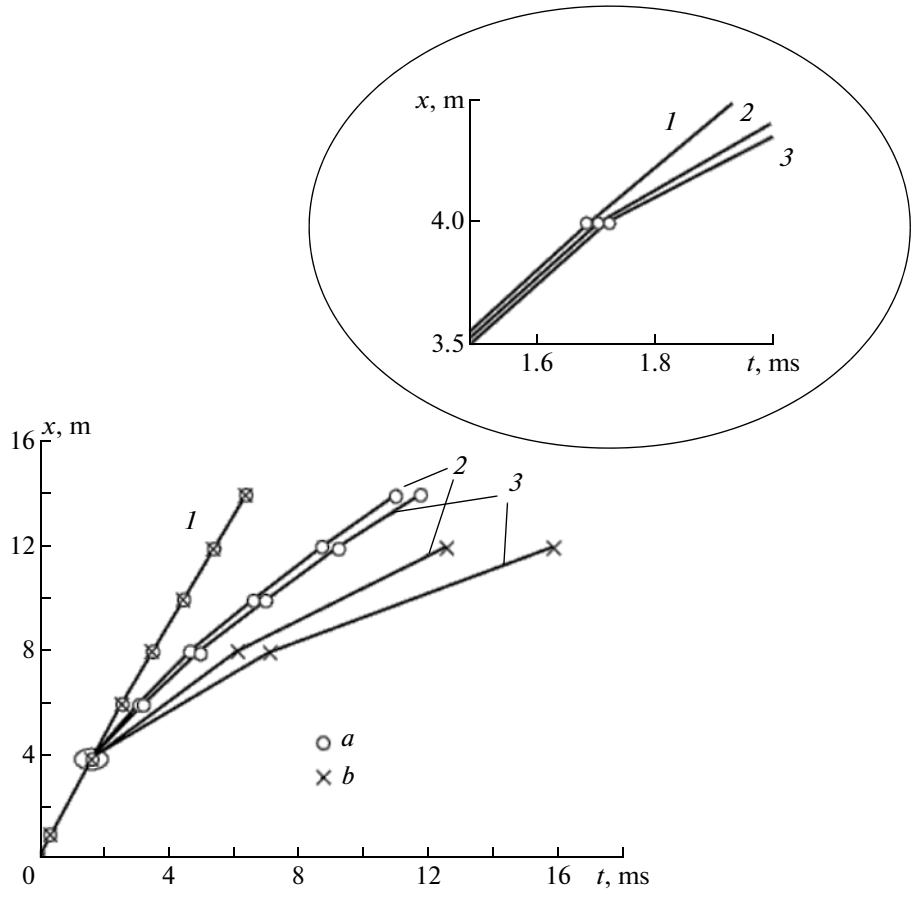

Fig. 13. Distance–time diagram for (*a*) shock wave and (*b*) reaction front propagation in 45% H_2–air mixtures (*1*) without and (*2, 3*) with inhibitors: (*2*) 2.5 vol % propene and (*3*) 2.5 vol % isobutene [5].

front progressively lagged behind the shock wave. This fact cannot be explained by the effect of dilution of the mixture. Special experiments showed that, in order to suppress detonation, substantially higher concentrations of an inert diluent are needed. At lower inhibitor concentrations in the hydrogen–air mixture, detonation failure was observed at larger distances from the detonation section entrance. For example, after the introduction of 2.2 vol % isobutene, detonation failure was observed only at a distance of 8 m from the detonation section entrance (Fig. 12). Up to this point, the detonation velocity was virtually constant and close to the detonation velocity of the mixture without inhibitor. By the end of this segment, a hardly noticeable but rapidly increasing lag of the reaction front behind the shock wave, which also begins to slow down, is observed, and detonation fails.

In the mixtures containing 2 vol % inhibitor, the detonation velocity is virtually identical to that in the mixture without inhibitor up to a distance of 12 m from the detonation section entrance, after which the lag between the reaction front and the shock wave becomes noticeable, but detonation persists.

Figure 13 compares the efficiency of isobutene and propene as inhibitors. As can be seen, in the presence of isobutene, detonation fails earlier and more sharply than in the presence of the same amount of propene. Calculations within the framework of the kinetic scheme presented in Section 3 for a 45% H_2 –air mixture containing 2.5% C_3H_6 showed that a steady detonation wave could propagate in this mixture at $d < 60$ mm. The fact that detonation failed in a 101-mm-diameter tube is apparently associated with an approximate character of the model, in particular, with the absence of a number of reactions involving C_3H_6 in the kinetic scheme.

5. CONCLUSIONS

Thus, a mathematical modeling of the chemical inhibition of hydrogen–air mixtures was performed. It was demonstrated that the proposed one-dimensional model of detonation makes it possible to describe the main regularities of the influence of inhibitors on detonation waves within the framework of a chain-branching mechanism of hydrogen combustion. The calculation results were found to be in close agreement with the available experimental data. According to these results, inhibitors cause a narrowing of the concentration limits and an increase in the limiting tube diameter at which detonation propagation is still possible. The inhibitor was demonstrated to suppress detonation despite the fact that it gives rise to additional exothermic reactions and additional hydrogen oxidation steps. At the same time, a retardation of the process is observed, which manifests itself in an increase in the autoignition delay time and in a decrease in the atomic hydrogen concentration, the main chain carrier of the branching-chain reaction. The effect of an inhibitor is largely determined by the specifics of the temperature dependence of the rate of the branching-chain reactions radically differs from the Arrhenius law.

ACKNOWLEDGMENTS

This work was supported in part by the Russian Foundation for Basic Research (project no. 08-08-00068), the program no. 11 of the Presidium of the Russian Academy of Sciences, and State Contracts Nos. P502 and 02.516.12.6026.

REFERENCES

1. A. S. Sokolik, *Autoignition, Flame, and Detonation in Gases* (Akad. Nauk SSSR, Moscow, 1960; Israel Program for Sci. Translat., Jerusalem, 1963).
2. B. Lewis and G. Elbe, *Combustion, Flames, and Explosions of Gases* (Acad. Press, Orlando, FL, 1987; Mir, Moscow, 1968).
3. V. V. Azatyan, I. M. Naboko, V. A. Petukhov, et al., Dokl. Akad. Nauk **394**, 61 (2004) [Dokl. Phys. Chem. **394** (1–3), 1 (2004)].
4. V. V. Azatyan, V. A. Pavlov, and O. P. Shatalov, Kinet. Katal. **46**, 835 (2005) [Kinet. Catal. **46**, 789 (2005)].
5. V. V. Azatyan, D. I. Baklanov, I. S. Gordopolova, et al., Dokl. Akad. Nauk **415** (2), 210 (2007) [Dokl. Phys. Chem. **415** (1), 174 (2007)].
6. G. L. Agafonov and S. M. Frolov, Fiz. Goreniya Vzryva **30** (1), 92 (1994).
7. Ya. B. Zel'dovich, Zh. Eksp. Teor. Fiz. **10**, 542 (1940).
8. Ya. B. Zel'dovich and A. S. Kompaneets, *Detonation Theory* (Gostekhteorizdat, Moscow, 1955) [in Russian].
9. Ya. B. Zel'dovich, B. E. Gel'fand, S. M. Frolov, and Ya. M. Kazhdan, Fiz. Goreniya Vzryva **23** (1), 103 (1987).
10. R. Reid, J. Prausnitz, and T. Sherwood, *The Properties of Gases and Liquids* (McGraw-Hill, New York, 1966; Khimiya, Leningrad, 1982).
11. B. J. McBride, M. J. Zehe, and G. Sanford, *NASA Glenn Coefficients for Calculating Thermodynamic Properties of Individual Species* (Glenn Res. Center, Cleveland, Ohio, 2002), p. 273.
12. A. Fish, in *Proc. of the Intern. Oxidation Symp.* (Stanford Research Inst., 1967), vol. 1, p. 431.
13. D. N. Lordkipanidze, V. V. Azatyan, Z. G. Dzotsenidze, and M. D. Museridze, Fiz. Goreniya Vzryva **15** (1), 73 (1979).
14. E. T. Denisov and V. V. Azatyan, *Inhibition of Chain Reactions* (Gordon Breach, London, 2000).
15. V. V. Azatyan, K. I. Gaganidze, S. A. Kolesnikov, and G. R. Trubnikov, Kinet. Katal. **22**, 244 (1982).
16. L. S. Polak, M. Ya. Gol'denberg, and A. A. Levitskii, *Computational Methods in Chemical Kinetics* (Nauka, Moscow, 1984) [in Russian].
17. T. Shikauchi, S. Fukutani, and N. Kuniyoshi, Nihon Kikai J. **4**, 345 (1999).
18. D. Pawel, H. Vasatko, and H. Gg. Wagner, Report AF EOAR, 67–49 (Inst. Phys. Chemie, Gottingen, 1969).
19. R. Knystautas, C. Guirao, et al., in *Dynamics of Shock Waves, Explosions and Detonations*, Ed. by J. R. Bowen, N. Manson, A. K. Opperheim, and R. I. Soloukhin (AIAA Inc., New York, 1984), vol. 94, p. 23.